Dosimetry of the Dopamine Transporter Radioligand ^{18}F-FPCIT in Human Subjects

William Robeson, MA; Vijay Dhawan, PhD; Abdel Belakhlef, PhD; Yilong Ma, PhD; Von Pillai, BS; Thomas Chaly, PhD; Claude Margouleff, MS; David Bjelke, AAS; and David Eidelberg, MD

Center for Neurosciences, North Shore University Hospital, Manhasset, New York

This study was designed to evaluate the radiation dosimetry in human subjects for a new radiopharmaceutical, *N*-(3-^{18}F-fluoropropyl)-2β-carbomethoxy-3β-(4-iodophenyl)nortropane (^{18}F-FPCIT). The goal was to determine a limiting dose consistent with accepted guidelines for use in clinical studies and to compare the radiation burden with other agents such as ^{123}I-FPCIT, ^{18}F-fluorodopa, and ^{18}F-FDG. **Methods:** Dynamic PET scans of the urinary bladder were obtained in 6 subjects; 2 subjects had brain scans and 5 subjects had scans of the thorax or abdomen. Regions of interest were placed over composite images of each organ for which activity was visualized to generate time–activity curves. Doses were calculated from residence times using the MIRDOSE3 program. **Results:** The critical organ for dosimetry is the urinary bladder wall with a dose of 0.0586 ± 0.0164 mGy/MBq. The dose comes primarily (97.2%) from activity in the urinary bladder contents. The dose is lower than any of the other agents used commonly in PET to assess dopaminergic function. The effective dose equivalent (0.0120 mGy/MBq) is also lower than comparable compounds. **Conclusion:** ^{18}F-FPCIT has favorable dosimetry when compared with other agents used to study dopaminergic function. Doses as high as 853 MBq (23 mCi) may be given to adult patients and remain within accepted guidelines.

Key Words: *N*-(3-fluoropropyl)-2β-carbomethoxy-3β-(4-iodophenyl)nortropane; dosimetry; PET; dopamine transporter

J Nucl Med 2003; 44:961–966

Parkinson's disease (PD) is characterized by degeneration of dopaminergic neurons, resulting in loss of dopamine transporters in the striatum. A dopamine transporter radioligand, *N*-(3-^{18}F-fluoropropyl)-2β-carbomethoxy-3β-(4-iodophenyl)nortropane (^{18}F-FPCIT), has recently been developed to study dopaminergic function (*1*,*2*). FPCIT has been shown to quantify regional abnormalities in dopamine transporter function associated with PD and has been labeled with ^{123}I for SPECT and ^{18}F for PET (*3*–*8*).

Dosimetry estimations have been reported for ^{123}I-FPCIT demonstrating favorable biodistribution with the critical organ being the large intestine (*9*). This is expected for ^{123}I-labeled compounds and is related to the dynamics of bowel excretion. ^{18}F-Labeled compounds such as ^{18}F-FDG and ^{18}F-fluorodopa (^{18}F-FDOPA) have the urinary bladder wall as the critical organ associated with the dynamics of urinary excretion of the shorter half-life isotope (*10*,*11*). ^{18}F-FPCIT has the advantage of being imaged with PET, which permits absolute quantification of striatal uptake. This study was undertaken to determine the activity of ^{18}F-FPCIT that could be injected into patients for clinical studies without exceeding accepted dosimetry guidelines while, at the same time, permitting the acquisition of high-quality images.

PET also permits the absolute quantification of radioactivity within organs of interest as required to perform dosimetry evaluations. We have performed 13 dynamic PET studies on 12 subjects and determined uptake and clearance in organs that localize ^{18}F-FPCIT. The following organs were evaluated: bladder (6 studies), lungs (3 studies), heart muscle (3 studies), liver (4 studies), spleen (4 studies), kidneys (3 studies), brain (2 studies), and spine or trabecular bone (1 study). The remainder of the body was evaluated from the subject in whom all organs except brain were studied. These data have been used as input to the MIRDOSE program to determine radiation absorbed doses (*12*).

MATERIALS AND METHODS

Subject Population

Thirteen dosimetry evaluations were performed on 12 human subjects. One subject had both bladder and thorax or abdomen scans performed. Nine men and 3 women (age range, 23–75 y; mean ± 1 SD, 59.2 ± 14.5 y) were studied. With the exception of 1 young person, the age range matches the patient population normally studied for PD.

Urinary Bladder Scans

Six subjects had dynamic PET scans of the bladder. There was some variation among subjects with regard to how data were acquired but a typical scan session went as follows. The subject was injected intravenously with approximately 185 MBq ^{18}F-FPCIT. The subject was positioned in the Advance PET scanner (General Electric Medical Systems) and a 10-min transmission scan of the lower abdomen was obtained using a rotating pin ^{68}Ge source. The transmission scan was used for attenuation correction of the subsequent emission data. Emission scanning commenced

Received Sep. 16, 2002; revision accepted Feb. 12, 2003.

For correspondence or reprints contact: William Robeson, MA, North Shore University Hospital, Biomedical Research Building, Room 128, 300 Community Dr., Manhasset, NY 11030.

E-mail: robeson@nshs.edu

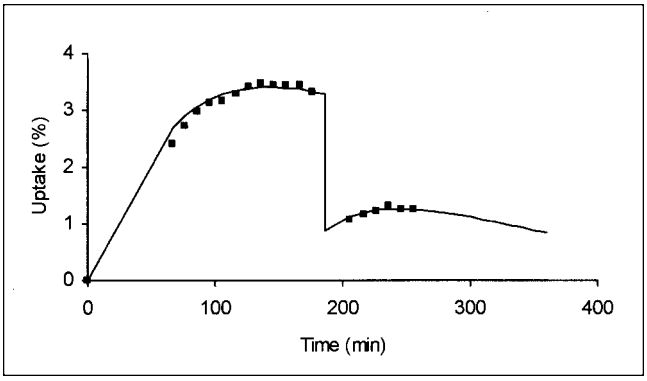

FIGURE 1. Bladder time–activity curve for subject 7. Data points reflect actual radioactivity measured by PET scanner scaled by measured urine concentration at approximately 180 min. Data are then further normalized by injected radioactivity. Solid line is fit to experimental data using exponential uptake and elimination by voiding and physical decay.

1 h after injection without moving the subject. Twelve 10-min dynamic scans of the bladder were obtained over the next 2 h. At 3 h after injection, the subject was removed from the scanner and sent to void. The urine was collected for assay of ^{18}F activity. The void volume was measured and recorded. Approximately 0.3 mL of urine was aliquoted and counted in a Canberra Series 20 well counter. Urine counts were background subtracted and corrected for well counter efficiency for ^{18}F (≈25%). The counts were then scaled to the void volume and the fractional injected activity in the void was determined. The patient was repositioned in the scanner and 6 additional 10-min scans were obtained.

The total study duration was approximately 4 h 15 min. The PET scans were reconstructed and analyzed by making a composite image set of all transaxial sections that contained the bladder. A region of interest (ROI) was drawn around the bladder and a time–activity curve was generated. The counts in the ROI were scaled to fractional injected activity using the measured data from the urine void (*11*). Time–activity curves were fit to a model of exponential uptake and elimination by voiding and physical decay. Figure 1 shows an example of a bladder time–activity curve from 1 subject. Residence times were calculated from the numeric integration of the curve. Only physical decay was considered beyond 6 h because no significant additional activity was assumed to enter the bladder.

Thorax or Abdomen Scans

Five subjects had dynamic PET scans of the thorax or abdomen. There was some variation among subjects with regard to how data were acquired, but a typical scan session went as follows. The subject was placed in the scanner such that the lungs, heart, liver, spleen, and kidneys could be visualized. This required operating the PET in scanning mode using 2 fields of view (FOVs). The axial extent of each 2 FOV scans was approximately 30 cm. The subject was injected with approximately 185 MBq ^{18}F-FPCIT and 14 dynamic scans were acquired over 2 h for both FOVs. The first 9 scans were acquired for 3 min in each FOV and the last 5 scans were acquired for 5 min in each FOV. Each FOV was acquired sequentially but there was approximately a 1-min gap between each dynamic scan. Emission data were corrected for attenuation using a 2-FOV transmission scan acquired without moving the subject. Emission data were reconstructed and composite transaxial images of each organ visualized were generated.

ROIs were drawn over parts of each organ. The ROIs were manually drawn by 2 of the investigators in such a way as to limit contributions from adjacent structures. For example, lung regions were drawn strictly on the right lung to avoid contribution from heart activity. The Advance scanner is calibrated to yield activity concentration directly from the scans. These values were converted to fractional organ uptake using Equation 1:

$$UPT = \frac{C_{PET}}{\rho_{ORGAN}} \times \frac{M_{ORGAN}}{A_{INJ}}, \qquad \text{Eq. 1}$$

where UPT is fractional uptake, C_{PET} is activity concentration (in kBq/mL), ρ is organ tissue density (in g/cm^3), M is organ mass (in g), and A is the activity injected into the patient (in kBq). Organ densities and masses are taken from the report of the task group on Reference Man (*13*). Time–activity curves were generated for the fractional uptake values for each organ for the 2-h period after injection. The tails of the curves were fit to a model of exponential elimination and the half-lives were calculated. Residence times were computed by numeric integration of the time–activity curves and the integrals were extrapolated to infinity using the calculated

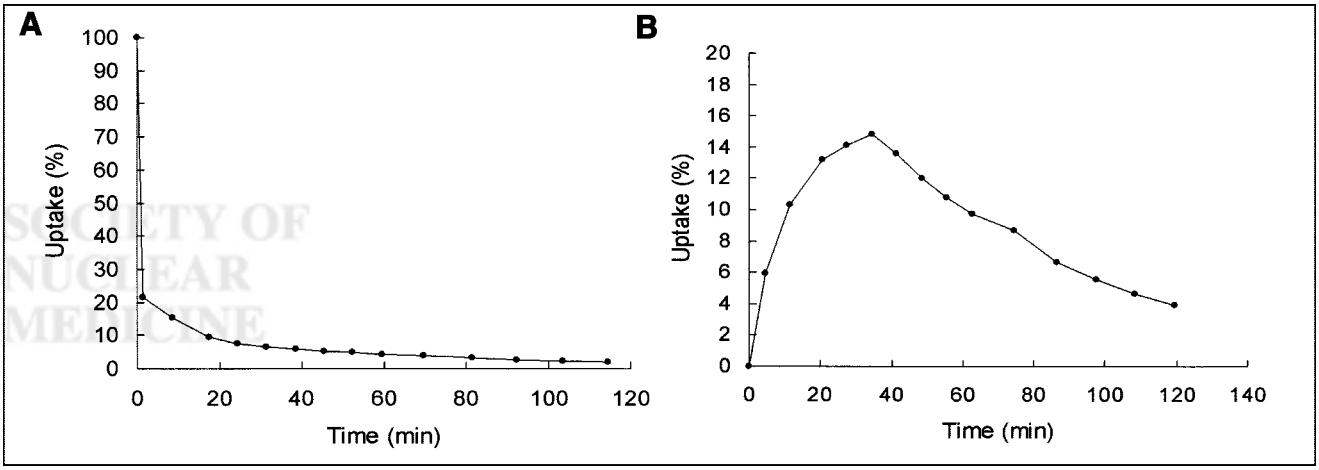

FIGURE 2. (A) Lung time–activity curve for subject 7. (B) Liver time–activity curve for subject 7.

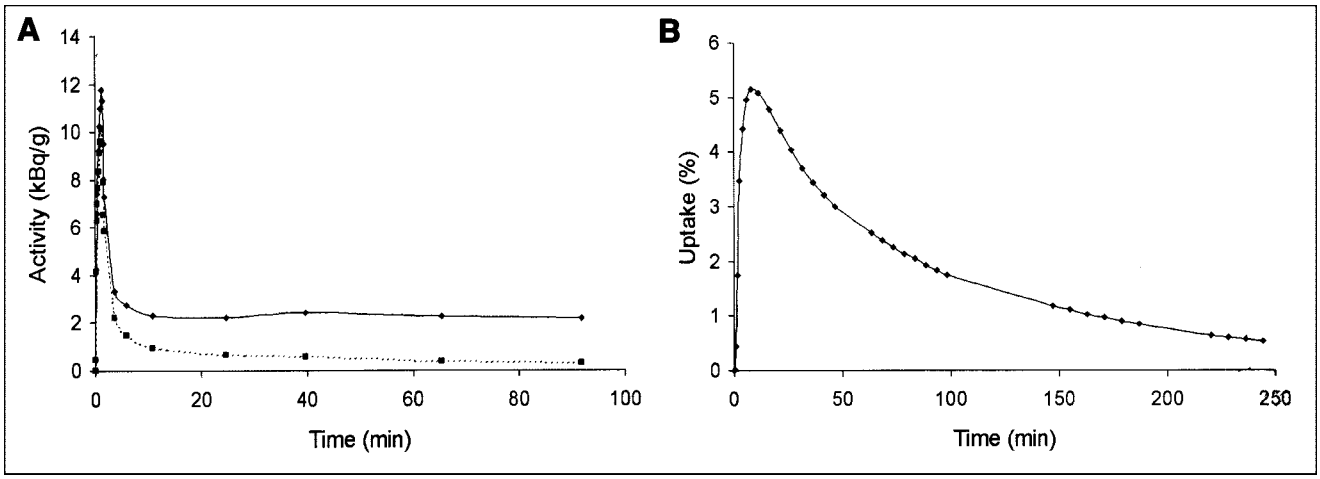

FIGURE 3. (A) Example of blood clearance curve for ^{18}F-FPCIT. Solid curve represents total ^{18}F in plasma. Dotted line is nonmetabolized ^{18}F-FPCIT determined by high-pressure liquid chromatographic separation of blood samples. (B) Brain time–activity curve for subject 12.

half-lives. Figure 2 shows examples of lung and liver time–activity curves from 1 subject.

Brain Scans

Two subjects had dynamic PET scans of the brain. There was slight variation between the 2 subjects with regard to how data were acquired, but a typical scan session went as follows. The subject was placed in the scanner such that the brain above the orbitomeatal line could be visualized. The subject was injected with approximately 185 MBq ^{18}F-FPCIT and 33 dynamic scans were acquired over 4 h. Emission data were corrected for attenuation using a transmission scan acquired without moving the subject.

Emission data were reconstructed and summed to create a composite transaxial image. An ROI was drawn over the entire brain. Average tissue concentration values were converted to fractional organ uptake using Equation 1. Time–activity curves were generated for the fractional uptake values for the 4-h period after injection. The curves were fit to a model of exponential uptake, and elimination and residence times were computed by integration of the time–activity curves (*14*).

Dosimetry Calculations

The average residence time was computed for each organ from among the subjects studied for that organ. These residence times were input into the MIRDOSE3 program to compute organ doses.

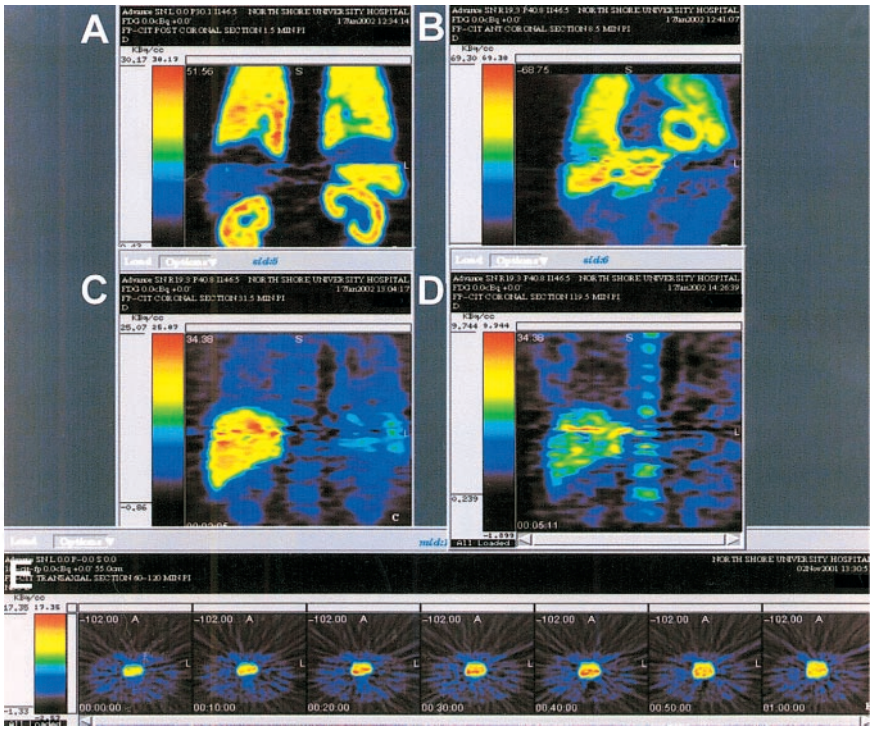

FIGURE 4. Uptake patterns of various organs as function of time for ^{18}F-FPCIT. (A) Coronal image of ^{18}F-FPCIT 0–6 min after injection shows early lung, spleen, and kidney uptake. (B) Coronal image of ^{18}F-FPCIT 7–13 min after injection shows cardiac muscle uptake. (C) Coronal image of ^{18}F-FPCIT 30–36 min after injection shows liver uptake and clearance from other organs. (D) Coronal image of ^{18}F-FPCIT 112–122 min after injection shows persistent spinal uptake and liver clearance. (E) Transaxial section of urinary bladder acquired at 7 time points from 1 to 2 h after injection shows growth of activity in bladder before patient voiding.

TABLE 1
Fractional Urinary Excretion of Injected Dose

Subject no.	% Excreted in urine
1	10.3
2	31.9
3	24.3
4	13.7
5	8.2
7	11.6
Average ± SD	16.7 ± 9.4

The ICRP 30 gastrointestinal (GI) tract model was used to estimate residence times for the intestines with input to the small intestine from liver clearance (*15*).

RESULTS

^{18}F-FPCIT is cleared rapidly from the blood. Figure 3A shows that unmetabolized ^{18}F-FPCIT falls to <10% of the injected dose within 15 min. Total ^{18}F activity falls below 25% in the same time interval. Figure 3B shows an example of brain uptake from 1 subject. Activity peaks within 10 min and clears biexponentially to approximately 10% within 4 h. Figure 4 demonstrates the uptake pattern of ^{18}F-FPCIT in other organs. Uptake in the lungs, heart, spleen, and kidneys peaks within the first 15 min after injection and clears rapidly from these organs. Liver uptake peaks at approximately 30 min and falls rapidly after that. Spinal uptake clears slowly and appears prominent out to 2 h.

Table 1 summarizes the fractional urinary excretion of the injected dose. Urine collections were obtained from the 6 subjects over a time interval ranging from 66 to 282 min after injection (mean ± 1 SD, 177.3 ± 77.1 min). The range of urinary excretion from 6 subjects was 8.2%–31.9% of the dose corrected for decay, with an average of 16.7% ± 9.4%. Table 2 summarizes the dynamics of liver uptake and clearance in 3 subjects. On the basis of the activity entering the liver and the transit time through the liver, 6.2% ± 1.5% of the administered activity is estimated to enter the GI tract. This value is used as input to the GI tract model to compute residence times in the intestines. Table 3 presents the computed organ residence times for each subject studied. One subject (subject 7) had time–activity curves generated for all organs evaluated in this article except the brain. Twenty-nine percent of the administered dose is accounted for from uptake in the heart, liver, spleen, kidneys, and trabecular bone. The remainder (71%) is assumed to be distributed uniformly in the remainder of the body.

The effective half-life is estimated at 88.8 min on the basis of the dynamics of bladder uptake. Residence times for the measured organs were consistent from subject to subject.

Table 4 presents the radiation dose estimates for the reference adult. The critical organ is the bladder wall, with a dose estimate of 0.0586 ± 0.0164 mGy/MBq. Approximately 97% of the dose is derived from activity in the urinary bladder contents. To limit the dose to 50 mGy to the critical organ, the maximum activity that may be administered is 853 MBq (23 mCi). For an administered dose of 853 MBq, the effective dose equivalent is estimated at 10.2 mSv. This is well below the guideline of 30 mSv established by our institutional radiation safety committee for human research subjects.

Table 5 presents comparative radiation dose estimates for ^{18}F-FPCIT with other radiopharmaceuticals used in the study of PD. The critical organ dose (bladder wall) and effective dose equivalent are lower than those of the other compounds. The radiation dose concern with ^{18}F radiopharmaceuticals is the bladder. One can compare the dose from ^{18}F-FPCIT with ^{18}F-FDOPA. For ^{18}F-FDOPA, approximately 10% of the administered activity appears in the bladder within 40 min after injection (*11*). With ^{18}F-FPCIT, only 3.5% appears in the bladder after 2.5 h (Fig. 1). The bladder dose for FPCIT, therefore, is only slightly greater than one third of that for ^{18}F-FDOPA (Table 5). The optimal voiding time for FPCIT appears to be 2–3 h after injection as opposed to 30–40 min after injection for ^{18}F-FDOPA.

DISCUSSION

The radioligand ^{18}F-FPCIT has favorable dosimetry associated with slower bladder clearance such that the critical organ (bladder) has a lower dose compared with other ^{18}F radiopharmaceuticals used to study dopaminergic function (Table 5). The bladder wall dose is approximately one half that associated with ^{18}F-FDG and slightly greater than one third the dose from ^{18}F-FDOPA. The intestinal dose is 15% of the same radioligand labeled with ^{123}I due to the shorter physical half-life. The

TABLE 2
Dynamics of Liver Uptake and Clearance

Subject no.	Peak liver activity (%)	Effective half-life (min)	Biologic half-life (min)	Transit time (min)	Activity entering GI tract (%)
7	14.8	45.0	76.3	110	7.4
9	19.0	56.4	116	167	6.6
10	12.0	53.9	106	153	4.6
Average ± SD	15.3 ± 3.5	51.8 ± 6.0	99.4 ± 20.6	143 ± 29.8	6.2 ± 1.5

TABLE 3
Residence Times

Subject no.	Age (y)	Sex	Residence time (min)								
			Bladder	Brain	Lungs	Heart	Liver	Spleen	Kidneys	Trabecular bone	Remainder
1	67	M	7.6								
2	72	M	13.2								
3	75	M	13.7								
4	72	M	8.5								
5	58	F	8.6								
6	52	M			8.7	1.0	10.0	0.7			
7	54	M	8.1		9.0	1.3	13.4	0.9	0.9	4.6	91.0
8	68	M			6.3	1.0					
9	67	F					22.7	0.6	0.4		
10	52	M					13.1	0.9	0.5		
11	50	M		4.3							
12	23	F		5.2							
Average	59.2		10.0	4.8	8.0	1.1	14.8	0.8	0.6	4.6	91.0
± SD	± 14.5		± 2.7	± 0.64	± 1.5	± 0.17	± 5.5	± 0.15	± 0.26		
Fractional SD	0.24		0.28	0.13	0.18	0.16	0.37	0.19	0.44		

average brain dose is low because ^{18}F-FPCIT localizes in the striatum with very rapid clearance from cortical structures. The effective dose equivalent is the lowest of all radiopharmaceuticals discussed in this article.

FPCIT is a new radiopharmaceutical with potential clinical usefulness in the diagnosis of PD. High target-to-background ratios have been exhibited with striatal-to-occipital uptake ratios of 3–4 in healthy subjects (*4*). The compound can be labeled with ^{18}F for PET studies or ^{123}I for SPECT studies. FPCIT demonstrates a decline in striatal uptake with age in healthy subjects and significant reduction in striatal binding in PD at the earliest stages of illness (*4,16*). ^{18}F-FDOPA quantifies the activity of dopa decarboxylase that is upregulated in residual dopaminergic neurons and, therefore, is not as sensitive in early-stage PD (*17*). Recent investigations have demonstrated faster kinetics with FPCIT and higher dopamine transporter selectivity than the original analog β-CIT (*5*). A single 10-min scan starting 90 min after injection provides a simple way to study PD mechanism and progression in clinical investigations (*18*).

TABLE 4
Radiation Dose Estimates for Reference Adult

Target organ	Total dose		Primary contributor	(%)	Secondary contributor	(%)
	mGy/MBq	rad/mCi				
Urinary bladder wall	5.86E−02	2.17E−01	Urinary bladder	97.2	Remainder of body	2.8
Lungs	1.92E−02	7.09E−02	Lungs	100		
Liver	1.86E−02	6.89E−02	Liver	100		
Small intestine	1.84E−02	6.82E−02	Small intestine	91.1	Remainder of body	8.9
ULI wall	1.84E−02	6.82E−02	ULI	91.1	Remainder of body	8.9
Spleen	1.02E−02	3.78E−02	Spleen	100		
Heart wall	8.20E−03	3.03E−02	Heart wall	100		
Brain	8.11E−03	3.00E−02	Brain	100		
Bone surfaces	6.74E−03	2.49E−02	Trabecular bone	72.8	Remainder of body	27.2
LLI wall	6.63E−03	2.45E−02	LLI	75.2	Remainder of body	24.8
Red marrow	5.11E−03	1.89E−02	Trabecular bone	50.7	Remainder of body	49.3
Kidneys	4.82E−03	1.78E−02	Kidneys	100		
Ovaries	3.29E−03	1.22E−02	Remainder of body	100		
Testes	3.29E−03	1.22E−02	Remainder of body	100		
Total body	4.40E−03	1.63E−02	Remainder of body	68.0	Liver	11.0
Effective dose equivalent	mSv/MBq	rem/mCi				
	1.20E−02	4.44E−02	Remainder of body	62.2	Lungs	19.2

ULI = upper large intestine; LLI = lower large intestine.

TABLE 5
Comparative Radiation Dose Estimates for ^{18}F-FPCIT with Other Radiopharmaceuticals Used in Study of PD

Organ	Comparative radiation dose estimates (mGy/MBq)			
	^{18}F-FPCIT	^{123}I-FPCIT*	^{18}F-FDOPA†	^{18}F-FDG‡
Bladder wall	5.86E−02	6.4E−02	1.59E−01	1.19E−01
Maximum intestine	1.84E−02	1.19E−01	1.14E−02	1.7E−02
Effective dose equivalent (mSv/MBq)	1.20E−02	4.1E−02	1.79E−02	3.0E−02

*Data from (*9*).
†Data from (*11*).
‡Bladder data from (*10*); intestine and effective dose equivalent data from (*19*).

CONCLUSION

^{18}F-FPCIT can be used to produce high-quality diagnostic images of the striatum in patients with PD with relatively low radiation burden. A standard clinical dose of 185 MBq (5 mCi) may be used to produce high-quality images (*4*). This dose is well below the 853-MBq (23 mCi) limiting dose proposed in this article.

REFERENCES

1. Abi-Dargham A, Gandelman MS, DeErausquin GA, et al. SPECT imaging of dopamine transporters in human brain with iodine-123 fluoroalkyl analogs of β-CIT. *J Nucl Med.* 1996;37:1129–1133.
2. Chaly T, Dhawan V, Kazumata K, et al. Radiosynthesis of [^{18}F] N-3-fluoropropyl-2-β-carbomethoxy-3-β-(4-iodophenyl) nortropane and the first human study with positron emission tomography. *Nucl Med Biol.* 1996;23:999–1004.
3. Seibyl JP, Marek K, Sheff K, et al. Iodine-123-β-CIT and iodine-123-FPCIT SPECT measurement of dopamine transporters in healthy subjects and Parkinson's patients. *J Nucl Med.* 1998;39:1500–1508.
4. Kazumata K, Dhawan V, Chaly T, et al. Dopamine transporter imaging with fluorine-18-FPCIT and PET. *J Nucl Med.* 1998;39:1521–1530.
5. Booij J, Hemelaar TG, Speelman JD, et al. One-day protocol for imaging of the nigrostriatal dopaminergic pathway in Parkinson's disease by [^{123}I]FPCIT SPECT. *J Nucl Med.* 1999;40:753–761.
6. Habraken JB, Booij J, Slomka P, et al. Quantification and visualization of defects of the functional dopaminergic system using an automatic algorithm. *J Nucl Med.* 1999;40:1091–1097.
7. Benamer HT, Patterson J, Wyper DJ, et al. Correlation of Parkinson's disease severity and duration with ^{123}I-FP-CIT SPECT striatal uptake. *Mov Disord.* 2000;15:692–698.
8. Ma Y, Dhawan V, Mentis M, Chaly T, Spetsieris PG, Eidelberg D. Parametric mapping of [^{18}F]FPCIT binding in early stage Parkinson's disease: a PET study. *Synapse.* 2002;45:125–133.
9. Abi-Dargham A, Innis RB, Wisniewski G, et al. Human biodistribution and dosimetry of iodine-123-fluoroalkyl analogs of β-CIT. *Eur J Nucl Med.* 1997; 24:1422–1425.
10. Jones SC, Alavi A, Christman D, et al. The radiation dosimetry of 2-[F-18]fluoro-2-deoxy-D-glucose in man. *J Nucl Med.* 1982;23:613–617.
11. Dhawan V, Belakhlef A, Robeson W, et al. Bladder wall radiation dose in humans from fluorine-18-FDOPA. *J Nucl Med.* 1996;37:1850–1852.
12. Stabin MG. MIRDOSE: personal computer software for internal dose assessment in nuclear medicine. *J Nucl Med.* 1996;37:538–546.
13. International Commission on Radiological Protection. *Reference Man: Anatomical, Physiological and Metabolic Characteristics.* ICRP Publication 23. New York, NY: Pergamon Press; 1975.
14. Sorenson JA, Phelps ME. *Physics in Nuclear* Medicine. 2nd ed. Philadelphia, PA: WB Saunders; 1987:200–206.
15. International Commission on Radiological Protection. *Limits for the Intake of Radionuclides by Workers.* ICRP Publication 30: Part 1. New York, NY: Pergamon Press; 1979.
16. Ishikawa T, Dhawan V, Kazumata K, et al. Comparative nigrostriatal dopaminergic imaging with iodine-123-βCIT-FP/SPECT and fluorine-18-FDOPA/PET. *J Nucl Med.* 1996;37:1760–1765.
17. Eidelberg D, Takikawa S, Dhawan V, et al. Striatal ^{18}F-DOPA uptake: absence of aging effect. *J Cereb Blood Flow Metab.* 1993;13:881–888.
18. Ma Y, Pillai V, Chaly T, et al. Parametric comparison of striatal ^{18}F-FPCIT uptake in Parkinson's disease [abstract]. *J Nucl Med.* 2002;43(suppl):56P.
19. Radiation Dose Estimates for Radiopharmaceuticals [on-line database]. Oak Ridge, TN: Radiation Internal Dose Information Center, Oak Ridge Institute for Science and Education; 1996. www.orau.gov/ehsd/ridic.htm. Accessed January 7, 1997.